Biophysical Chemistry, 39 (1991) 177–190

BIOCHE 01538

Determination of K^+-channel relaxation times in squid axon membrane by Hodgkin-Huxley and by direct linear analysis

Harvey M. Fishman [a] and Raymond J. Lipicky [b]

[a] *Department of Physiology and Biophysics, University of Texas Medical Branch, Galveston, TX 77550 and* [b] *Division of Cardio-Renal Drug Products, Office of Drug Evaluation I, CDER, Food and Drug Administration, Rockville, MD 20857, U.S.A.*

Received 10 May 1990
Revised manuscript received 30 August 1990
Accepted 10 September 1990

Hodgkin-Huxley analysis; Rapid admittance analysis; K^+-channel macrokinetics; Small-signal analysis; (Squid axon)

An assumption in the use of the Hodgkin-Huxley (HH) formulation (A.L. Hodgkin and A.F. Huxley, J. Physiol. 117 (1952) 500) to extract kinetic parameters from ion conductance responses to step voltage changes across biological membranes is that estimates obtained from such an analysis are equivalent to those obtained by direct, small-perturbation analysis. Comparison of the estimates of the K^+-conductance relaxation time, τ_n, derived from HH vs rapid, complex admittance determinations in the same squid giant axons shows significant differences for the same step changes over a 60 mV range from holding (−65 mV). The admittance determinations (2.5–5000 Hz) are shown to satisfy criteria of linear analysis (i.e., estimates are equivalent to a small-step analysis and are time invariant). The discrepancies between the two methods arise from the fact that the HH power-law description for a constant power does not yield a best fit of data over the voltage range examined and thus best estimates of τ_n are power dependent. Furthermore, the large step changes in membrane voltage may excite nonlinear modes unrelated to conductance gating that contaminate the data to which the nonlinear formulation is applied to estimate linear kinetic parameters. Thus, the long-standing assumption that application of the HH methodology and empiricism is equivalent to a direct linear analysis is not substantiated. This result suggests that in comparisons between microscopic and macroscopic conduction data, microkinetic parameters derived from analysis of single ion-channel data should not be compared to macrokinetic parameters from a large population of the channel derived by HH analysis.

1. Introduction

Application of the Hodgkin-Huxley (HH) methodology [1] and their empirical power-law formulation to characterize electric-field dependent ion channel conduction in biological membranes has become the conventional way in which to describe the macrokinetics of these membrane processes. To obtain a description of K^+ conduction the HH procedure consists of suppressing Na^+ conduction and successively stepping the membrane potential ('voltage clamps') from a quiescent holding value (at which the mean current is small) to a range of physiological values to obtain the time course of the membrane ionic current (after an initial, rapidly decaying capacitive transient) in response to each step. The set of relatively large (> 10 mV) step clamps elicit nonlinear responses that are fitted by the HH formulation, which assumes underlying linear kinetics for the K^+-conductance rate process and a nonlinear K^+ conductance via a power-law dependence on a parameter, n, of the rate process. From a curve fit of the nonlinear response to each step

Correspondence address: H.M. Fishman, Dept. of Physiology and Biophysics, University of Texas Medical Branch, Galveston, TX 77550, U.S.A.

voltage, linear kinetic parameters associated with the K^+-current time course are obtained.

An implicit assumption of the HH methodology is that kinetic parameters, e.g., the relaxation time of the conductance, obtained from such an analysis are equivalent to those obtained from a direct ('small signal') linear analysis. With the advent of methods for rapid determination of the small-signal admittance of membranes [2–5], a direct linear analysis of ion conduction in membranes is now possible [4,6,7], and the assumption that an HH analysis is equivalent to a direct linear analysis became testable.

One may well ask, in light of the patch-clamp technique [8] which provides microscopic conduction information directly, why the above question is of importance. A prime reason is that a proper macrokinetic description is critically important in relating microscopic information to the macroscopic properties of ion channels. For example, in order that comparisons be meaningful, the relaxation times obtained from fits of sums of exponential functions (Markov modeling) to open- and closed-time distributions of single-channel currents [9] should be compared to the relaxation times, derived from a truly linear analysis, of the conductance of a large population of identical channels. Furthermore, in light of abnormal and variable stresses placed upon channels in a patch of membrane isolated in a glass micropipette [10] and the possibility that Markovian kinetic schemes may only be an approximation to inherently nonlinear rate processes [6,11], a comparison of microscopic data with a proper linear macroscopic description may be an important way to decide whether acquired microscopic data relate to macroscopic processes.

In this study we compare the relaxation times, $\tau_n(V)$, of outward, 'delayed rectifier' K^+ channels in the squid axon membrane, derived from fits of the HH K^+-current relation to step voltage-clamp current responses, with estimates of τ_n from curve fits of an admittance model [12–14] from linearized HH equations [1] to the membrane complex admittance, determined in a steady state (200 ms after step clamps). The main result is that the estimates of τ_n obtained from the HH methodology do not agree with those from a direct linear analysis via membrane admittance determinations. Preliminary reports of this work have appeared [15,16].

2. Materials and methods

2.1. Preparation and solutions

Giant axons from the hindmost stellar nerve of squid (*Loligo pealei*) were used in these experiments. Conventional, internal, axial-electrode techniques, as described previously [6], were implemented. The external solution was an artificial seawater (ASW) composed of (in mM) 430 NaCl, 10 $CaCl_2$, 50 $MgCl_2$, 20 sucrose and 5 Tris-Cl buffered to pH 7.4 at 22°C. Tetrodotoxin (TTX) (1 μM) was added to the ASW in all experiments described in order to eliminate Na^+ conduction. In experiments in which measurements were made during internal perfusion of an axon, the internal perfusate was composed of (in mM) 295 KF, 330 sucrose and 5 Tris-Cl, buffered to pH 7.4 at 22°C.

2.2. Voltage clamp and chamber

The voltage-clamp system was optimized for speed of response with a voltage response rise-time to a step command of less than 1 μs. Membrane capacitance charged with a time constant of about 6 μs. Current measurements were made from approx. 4-mm lengths of axon bathed in cooled, flowing ASW in the central compartment of a chamber divided into three compartments by two thin partitions. The axon extended from the central compartment through a hole in each partition (0.1 mm thick Mylar) for 6 mm in air on both sides of the central compartment. One or two drops of a solution of 0.8 M sucrose plus TTX (1 μM) were applied to each axon segment in the air gaps to reduce substantially 'end effects' in the centrally measured current. In the case of intact axons (no internal perfusion), experiments were begun after the axon in the air gaps had dried, as demonstrated by a significant reduction in the apparent leakage current. In internally perfused axons [6], experiments began after stabilization of the leakage

and step clamp currents (10–20 min after initiating perfusion).

2.3. Electrical measurements

Three types of measurements were made for comparison purposes. Conventional, large-step (> 10 mV) current responses were obtained. For small steps (< 10 mV) from holding potential (−65 mV), signal averaging of repetitively evoked current responses was implemented to enhance signal-to-noise performance.

The second type of measurement was complex admittance determinations, which were made by superposing a small-amplitude (1 mV, r.m.s.), Fourier-synthesized signal onto large step clamps [4,14,18]. In these experiments, to enhance the accuracy of admittance determinations at each membrane potential, the real and imaginary parts of three or eight successively acquired admittance functions were averaged at each frequency. From the averaged real and imaginary parts at each frequency, an averaged admittance function, which was used for curve fitting, was computed.

In a third type of measurement, a 1 mV step was substituted for the small, synthesized signal in order to obtain the small-step response in the same acquisition interval (see fig. 3A) as that in which the admittance was determined. This allowed comparison of the relaxation times from the admittance data with those obtained from analysis of the small-step current response acquired with exactly the same premeasurement interval and conditions. For the comparison of admittance and small-step response data, both of these measurements were made in the same axons with a separate low-noise voltage-clamp system, described previously [6].

To minimize effects due to nonstationarity of the preparation during different measurements, all data types from which estimates of relaxation times were to be compared were obtained at each membrane potential before proceeding to the next membrane potential. Usually only two of the three types of measurements could be completed at 12 different membrane potentials before significant change in membrane relaxation times occurred.

2.4. Compensation for series resistance

Compensation for 2.7–3 Ω cm^2 of series resistance was made during acquisition of step voltage-clamp data. The value of compensation was determined from the asymptotic approach to 'infinite' frequency of the impedance locus in the complex plane (plot of real vs imaginary parts of the impedance at each frequency) in the frequency range 125 Hz–50 kHz. The impedance determination used the same synthesized signal technique as described for rapid impedance measurements [14] except that the signal was applied as a constant current stimulus and the membrane voltage response was analyzed with respect to the stimulus. No compensation was made for series resistance during acquisition of admittance data under voltage clamp because the voltage drop across the series resistance was less than 1.5 mV for the largest step used. In addition, these measurements were made in a steady state and thus series resistance was included in the admittance model used to fit the data.

2.5. Data analysis

The HH formulation defines potassium current, i_K, flow through the membrane as

$$i_K = \bar{g}_K n^4 (V - E_K) \quad (1)$$

where $\bar{g}_K$ denotes the maximum attainable conductance when all K^+ channels are conducting, n is a voltage- and time-dependent activation parameter which takes on values from 0 to 1 (i.e., the fractional part of the potassium conducting system that participates in conduction), V represents the voltage difference across the membrane, and E_K is the potassium equilibrium potential. The exponent on n was chosen empirically to be 4 so that the membrane current response to step voltages would have an initial, variable 'induction phase' (delay) that gives the response a sigmoidal shape. HH also assumed the kinetics of the n process to be first order and described by the rate equation

$$\frac{dn}{dt} = \alpha_n(1 - n) - \beta_n n \quad (2)$$

where α_n and β_n are thought of as forward and backward rate constants of a two-state process associated with the subunits of a K^+ channel. The response of eq. 2 to a voltage step is

$$n(t) = n_\infty - (n_\infty - n_0)\exp(-t/\tau_n) \quad (3)$$

where $\tau_n = (\alpha_n + \beta_n)^{-1}$, and the subscript ∞ refers to the steady-state value after establishment of a new membrane potential and 0 to the initial value of n at the former membrane potential. Substitution of eq. 3 into eq. 1 yields an equation of the following form:

$$i_K = I_{K_\infty}[1 - B_n \exp(-t/\tau_n)]^x \quad (4)$$

where $I_{K_\infty} = \bar{g}_K n^x (V - E_K)$ and $B_n = (n_\infty - n_0)/n_\infty$. Eq. 4 was used to fit the step responses after correction for leakage and removal of capacitive transients. Four parameters, I_{K_∞}, B_n, x and τ_n, were varied so that the exponent, x, for the best fit (least-squares criterion) could be determined.

The sensitivity of the estimate of τ_n on x was examined by comparing the value of τ_n obtained for the best fit of the data with a fixed exponent [$x = 4$ (HH)] with the value obtained for fits with x variable. Eq. 4 was also used to fit the small-step (1 mV) responses [18] obtained after the same premeasurement interval (fig. 3A) used in the acquisition of admittance data.

Complex admittance determinations were fitted by an admittance function [12–14] based on the linearized HH equations [1]. Admittance measurements were made under steady-state conditions (see section 3.4). The measured complex admittance, $Y(jf)$, is given by

$$Y(jf) = [R_s + Y_m^{-1}(jf)]^{-1} \quad (5)$$

where j denotes the imaginary quantity $(-1)^{1/2}$ and f is frequency. The membrane admittance, $Y_m(jf)$, is due to capacitance, leakage and K^+ conduction and was modeled by

$$Y_m(jf) = (j2\pi f)^\theta C_m + g_L + Y_K(jf) \quad (6)$$

and

$$Y_K(jf) = g_{K_\infty} + g_K(1 + j2\pi f\tau_n)^{-1} \quad (7)$$

where C_m denotes membrane capacitance, θ is a number less than unity that reflects the constant-phase-angle character of C_m [19], g_L is the leakage conductance, g_{K_∞} the potassium-system chord conductance, g_K the kinetic component of the K^+ conductance and τ_n is the relaxation time of g_K, to be compared with the τ_n obtained from the HH analysis of step-clamp current responses.

The step-clamp response, curve-fitting Fortran program TIMFIT used the grid search (GRIDLS [20]) method of least squares to explore the parameter space of the function in eq. 6. The parameter values that yielded the best fit (minimum χ^2 value) was obtained by minimizing χ^2 with respect to each parameter separately. While this method may converge very slowly toward a minimum if the variation of χ^2 with each parameter is not independent of how well the other parameters are optimized, the method is stable, simple and does converge. A useful addition to test for a local minimum was, upon approach to a minimum χ^2, to reset the incremental step size of each parameter to 10% of its value and to resume fitting. This perturbation usually produced sufficient change in the parameter space to proceed to a deeper minimum χ^2 if the prior one was only a local minimum.

The Fortran program CPXFIT that fitted eqs 5–7 to complex admittance data employed the same grid search method that was used in TIMFIT. However, because the admittance consists of two functions (i.e., the real and imaginary parts) of frequency, the χ^2 was minimized with respect to the vector (formed by the real and imaginary values at each frequency) difference between data and model.

Admittance data (points) are plotted in two ways: (i) as magnitude, $|Y(jf)| = [G^2(f) + B^2(f)]^{1/2}$, and phase $\angle Y(jf) = \tan^{-1}(B(f)/G(f))$, functions of frequency (12.5–5000 Hz) and (ii) as the reciprocal admittance in the complex impedance, $Z(jf) = R(f) + jX(f) = Y^{-1}(jf)$, plane [$X(f)$ vs $R(f)$]. Solid curves in each figure are the best fit of eq. 5 to the data with all quantities variable in the approach to the best fit. The best fit of the measured admittance of a five-electrical element circuit model gave estimates of fit parameters that were within 3% or less of the

actual values of each of the five electrical elements used in the circuit model.

3. Results

3.1. Comparison of $\tau_n(V)$ derived by HH and by admittance analysis of data from the same axon

Does the HH methodology produce estimates of τ_n that are equivalent to the values obtained on the same axon and under the same experimental conditions by a direct linear analysis from admittance determinations? To answer this question fig. 1 compares the results from such data analyses, which are similar to those obtained in 15 other axons. Clearly, the estimated $\tau_n(V)$ curve obtained from admittance determinations is different from that with a variable exponent, x in eq. 4 (the best fits of the temporal responses) or those with a fixed exponent of 4. Generally, the admittance yielded larger values for τ_n at the peak of the curve (in the membrane potential range -70 to -40 mV) than those from an HH analysis. One factor contributing to this result for relatively small-step changes (< 10 mV) from holding voltage is that curve fits of eq. (4) (with $x = 4$) to data were poorer (see fig. 2) than those in which x was variable. At more depolarized voltages (fig. 1) the admittance- and HH-derived $\tau_n(V)$ curves cross. Even at voltages approaching 0 mV the $x = 4$ curve underestimates the value of τ_n obtained for x variable (best fits) because an exponent of 4 did not yield good fits unless large steps (approaching 100 mV) were applied. One expects the 60 mV voltage range from holding in which the HH fits are poor to be very important because, in a current-driven preparation, the approach to threshold for impulse generation in which the transition from linear to nonlinear conduction is explosive-like in this voltage range.

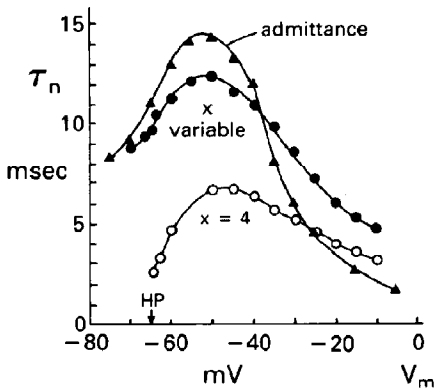

Fig. 1. Comparison of $\tau_n(V)$ estimates derived from fits of eq. 4 to step clamp i_K responses shown in fig. 2, with exponent, x, variable (filled circles) and fixed (HH) at 4 (open circles) with estimates derived from fits of eq. 5 (linear analysis) to admittances, shown in fig. 3B, (filled triangles) acquired 0.2 s after step clamps, as in fig. 3A. All data were obtained in the same intact (not internally perfused) axon under the same conditions.

Although the $\tau_n(V)$ curve with variable exponent in fig. 1 is closer to the admittance-derived curve, it still differs significantly. This means that values for τ_n from an HH analysis do not correspond to those obtained from a truly linear analysis. Clearly then, because the τ_n values obtained from an HH analysis depend on the value of exponent chosen to fit step responses and no single value fits data well over a 60 mV range from holding and because the relaxation times obtained from the best fits are not equivalent to those derived from a direct linear analysis, $\tau_n(V)$ determined from an HH analysis appears to be unrelatable to linear theory. Because of the discrepancy between HH- and admittance-analysis estimates of τ_n and the implications of this finding, the subsequent results focus on the analyses of the two types of data so that the reader may understand how the estimates presented in fig. 1 were obtained and assess the quality of the data and curve fits.

3.2. Estimate of the relaxation time, τ_n, dependence on voltage via the HH method

In order to apply eq. 4 to total current responses obtained from step voltage clamps of squid axon membrane, the capacitive and leakage components of current were removed from the total response to yield $i_K(t)$. In curve fitting the K^+-current responses, the value of the exponent, x, in eq. 4 that gave the best fit of these curves varied significantly with voltage ($x = 1.3$ at -60 mV to

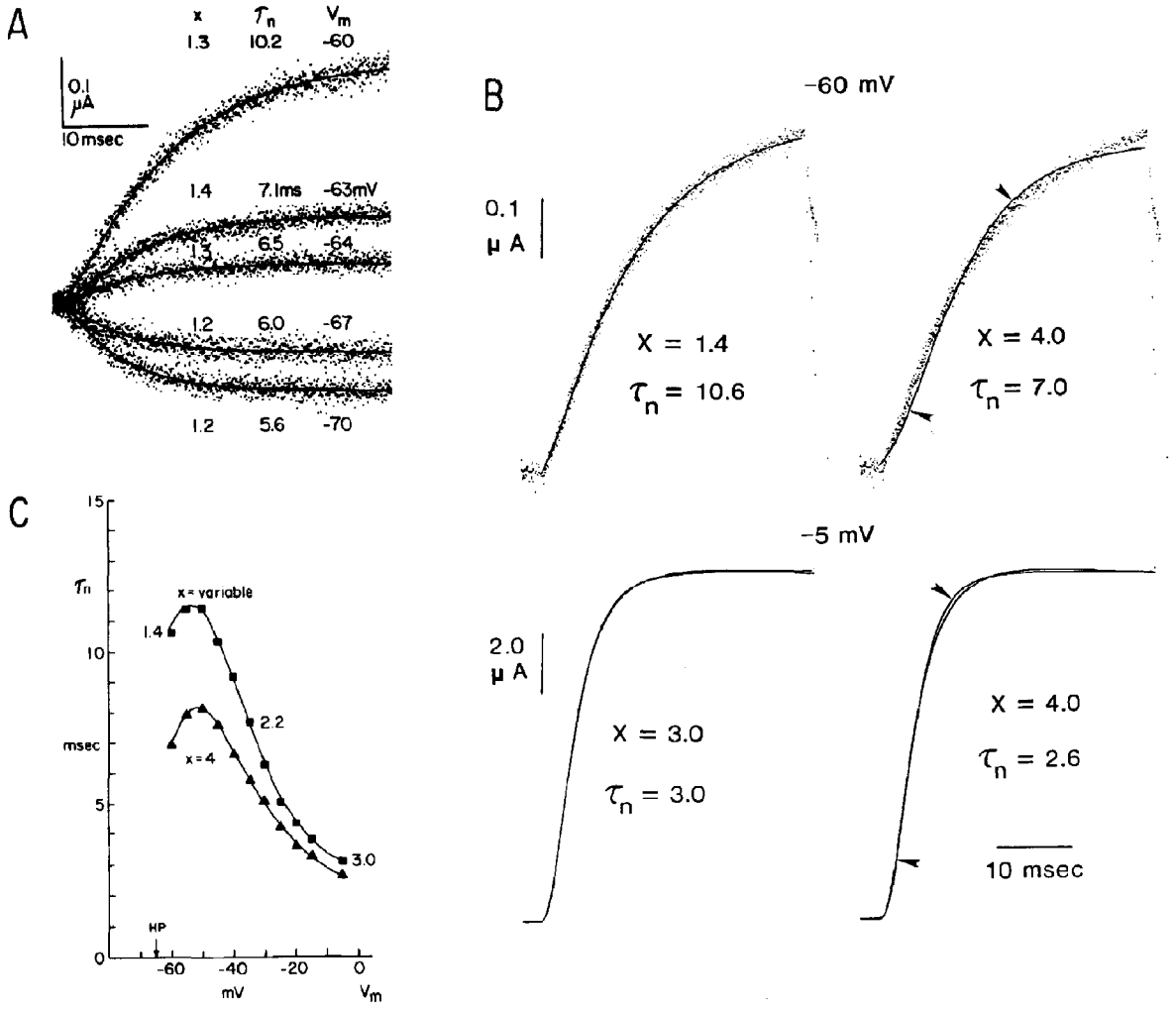

Fig. 2. (A) Small-step response of K^+ conductance together with the best curve fits (solid curves) of eq. 4, yielding values of x and τ_n for the best fit of each response for steps from holding (−65 mV) to the voltages indicated. Note that for these small-step responses the exponent for best fits approaches that of a first-order relaxation ($x = 1.0$, with no delay [18]) and consequently, fits with an HH exponent of 4 were poorer. Data points are averages from 25 evoked responses for steps of −5, −2, 1 and 2 mV and from 16 responses for the step of 5 mV from holding. The external solution was ASW + TTX (1 μM) in intact axon 86–60; 11.3° C; membrane area = 0.05 cm^2. (B) Comparison of HH model fits of the capacitive transient- and leakage-corrected K^+-current response to a relatively small (5 mV) and a large (60 mV) step from holding (−65 mV) to membrane potentials −60 and −5 mV, respectively. The best fits of eq. 4 in the potential range between these two steps were obtained with the exponent, x, variable. Fits with $x = 4$ were not good until step sizes approached 100 mV. Note (arrowheads) that the HH fits (for $x = 4$) initially rise too slowly and subsequently rise too rapidly with respect to the data. This is best seen in the curve fit for a step to −60 mV. This kind of misfit was characteristic of eq. 4 with $x = 4$ throughout the potential range from −60 to −5 mV. Intact axon 86–54 ASW + TTX (1 μM); 11.7° C; membrane area = 0.04 cm^2. (C) K^+-conductance relaxation time as a function of voltage, $\tau_n(V)$, derived from best fits of eq. 4 to squid axon voltage-clamp responses with exponent, x, variable (filled squares) and fixed at 4 (filled triangles). As indicated in panels A and B, fits with x variable (in the range 60 mV depolarized from holding of −65 mV) were invariably better than the best fits with $x = 4$. Estimates are from step response data obtained on the same axon as in panel B.

$x = 3.4$ at -30 mV). Generally, the value of the exponent for best fit of the responses increased monotonically from 1 to 3 with increasingly larger depolarizations. To examine this aspect more closely, small-step (between +5 mV) responses from a holding potential of -65 mV were obtained by signal averaging evoked responses at each potential. These small-step K^+-current responses are shown in fig. 2A. The solid curves in fig. 2A are the best fits of eq. 4. The values for x and τ_n from these fits at step voltages of 1, 2, 5, -2 and -5 mV from holding (-65 mV) are tabulated in fig. 2A. The value of x for these responses to small steps ranged from 1.2 to 1.4, significantly lower than the HH value of 4 but consistent with previous findings [18] that as step size is decreased below 1 mV the initial delay disappears and the response becomes first order (i.e., x approaches 1).

The i_K responses to large steps were also curve fitted to obtain best fits. For comparison, fits of the same responses with the HH value of $x = 4$, held constant regardless of step voltage, were made. Fig. 2B shows this comparison at two potentials, namely, steps to -60 and to -5 from a holding of -65 mV. For the small step of 5 mV the two fits (solid curves) to the response show that the HH exponent of 4 produces a curve that initially rises too slowly and then crosses the latter part of the curve twice. This fitting pattern was repeated for the responses at increasing step potentials, as seen in the fit of the response to a 60 mV step to -5 mV in fig. 2B. However, for larger steps approaching 100 mV, the fit of i_K responses by eq. 4 with an exponent of 4 was improved. Nevertheless, at -5 mV the best fit only required an exponent of 3. Invariably the best fits over the entire potential range examined were obtained by letting the exponent vary.

The above points for all of the data collected are summarized in the graph of fig. 2C. Fits of the responses to 11 steps covering the membrane potential range from -60 to -5 mV were obtained. The values for the K^+-conductance relaxation time, τ_n, obtained from these fits are plotted vs potential for the best fits (exponent x variable) and for HH fits ($x = 4$ irrespective of voltage). The displacement between the curves over the entire potential range indicates that an exponent of 4 does not yield the best fit of data in this range. Furthermore, the variation in x from 1.4 to 3 for the best fit of responses in this voltage range means that no single value of exponent, x, in eq. 4 yielded good fits of step-clamp data over a 60 mV potential range depolarized from holding (-65 mV). The empiricism associated with the value of the exponent leads to the result that $\tau_n(V)$ evaluated by the HH formulation depends on the particular value chosen, which if held constant does not yield the best fit of data over the potential range from -60 to -5 mV.

3.3. Estimate of $\tau_n(V)$ from model curve fits of membrane admittance determinations

Fig. 3A illustrates the acquisition of admittance data during a rectangular voltage-clamp pulse. The horizontal, dashed line with periodic vertical marks indicates the start of a continuously applied, repetitive, 1 mV signal. A large voltage step (30 mV), from -65 to -35 mV, was applied so that the response to the small (1 mV), synthesized signal occurred after a specified premeasurement interval (200 ms in the illustration) and so that one complete cycle of the signal (during the data acquisition 'window' in fig. 3A) began precisely after the premeasurement interval. The small amplitude of the synthesized signal was necessary to ensure that the response containing the admittance information reflected primarily the linear properties of the membrane [18]. The premeasurement interval allowed the membrane to respond to several cycles of the perturbation signal before the data were acquired. The latter condition satisfies the additional requirement that data be obtained in a steady state in order that the frequency structure of the admittance not depend on the time of measurement and thus is interpretable in terms of linear time-invariant processes. In this respect, the frequency components introduced into the admittance function by the slow decaying phase of the mean-current response in fig. 3A were also eliminated in the time domain. This was done by a coherence elimination method described previously [4] in which a pair of evoked responses was obtained with an inversion (polarity change) of

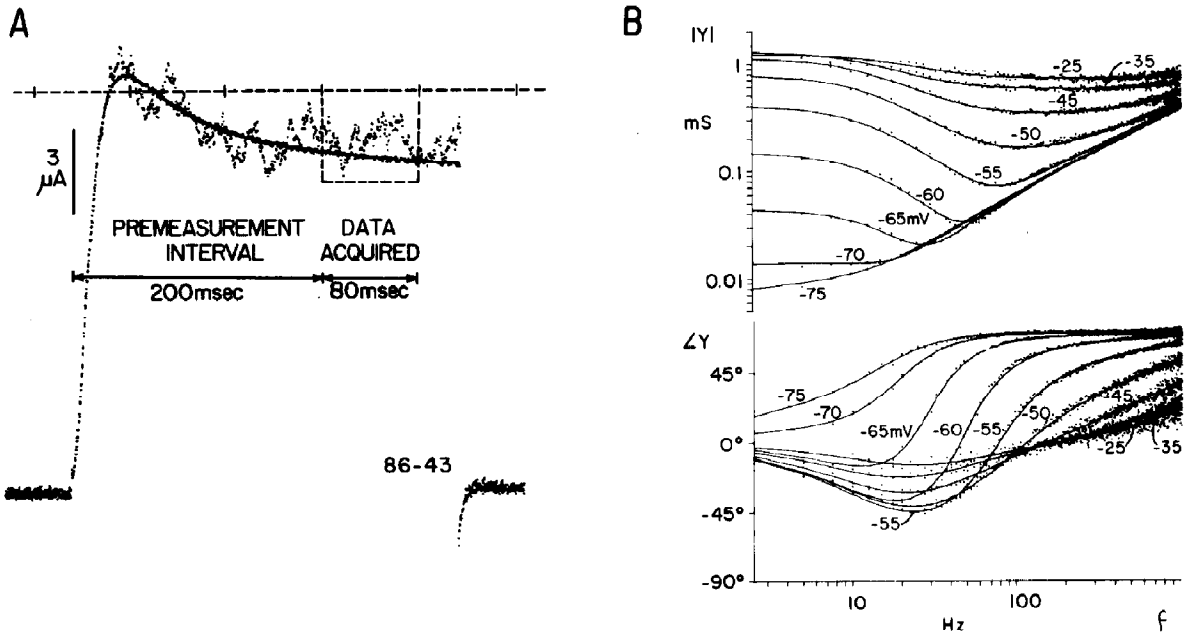

Fig. 3. (A) Illustration of the acquisition of admittance data during a voltage-clamp step. The current response to a repetitive, 1 mV (r.m.s.) Fourier-synthesized signal is acquired after a 'premeasurement interval' (200 ms) from the onset of an applied voltage step from −65 to −35 mV with the synthesized signal superposed and applied continuously with a periodicity indicated by the ticks on the dashed horizontal line. The data, from which the admittance was calculated, was acquired ('data acquired') in the dashed 'window', the duration of which (80 ms, in the example shown) depends upon the frequency resolution and range (in this example 12.5 and 5000 Hz, respectively) of the admittance determination. The premeasurement interval could be set to any value from 1 ms to 1 s by a sequencer (implemented by a microprocessor) that initiated the step clamp pulse at a time prior to the window and within the signal period so that a complete cycle of the signal began and ended within the desired data acquisition interval. The axon (86–43) was intact and bathed in a cooled, flowing solution of ASW plus TTX (1 μM); membrane area = 0.055 cm^2. (B) Magnitude and phase angle of membrane admittance, $Y(jf)$, in the frequency range 2.5–5000 Hz acquired, as illustrated in panel A, with a premeasurement interval of 0.2 s after step clamps to the membrane voltages indicated. The solid curves are the best fits (least-squares criterion) of eq. 5 with all parameters variable in the approach to each best fit. From these fits estimates of K^+-conductance relaxation time, τ_n, were obtained and are shown in the curve labeled admittance in fig. 1. Intact axon 86–57 in ASW + TTX (1 μM); 11.2° C.

the superposed, synthesized signal between acquisition of the paired responses. Time-domain subtraction of the pair of responses eliminated the decaying phase in the mean current, which was common to both large response pairs, while the admittance-containing small response was reinforced in the subtraction because of the intentional inversion of the small signal between response pairs.

Fig. 3B shows a set of admittance data and curve fits graphed as magnitude and phase angle functions of frequency. From the curve fits of eq. 5, estimates of τ_n, plotted in fig. 1, were obtained from these data.

3.4. Determination of the time after a step clamp in which the membrane admittance is in steady state

Rapid admittance determinations in biological membranes can be used to characterize the linear response of membrane conduction [4,6,7,11,14] provided that: (i) the amplitude of the voltage stimulus elicits an insignificant nonlinear response (harmonics) and (ii) the admittance determination is invariant with time. With respect to (i), the amplitude of the voltage perturbation used to elicit the admittance data at any given membrane potential in these experiments was chosen to be 1 mV (r.m.s.), which was shown previously [18] by

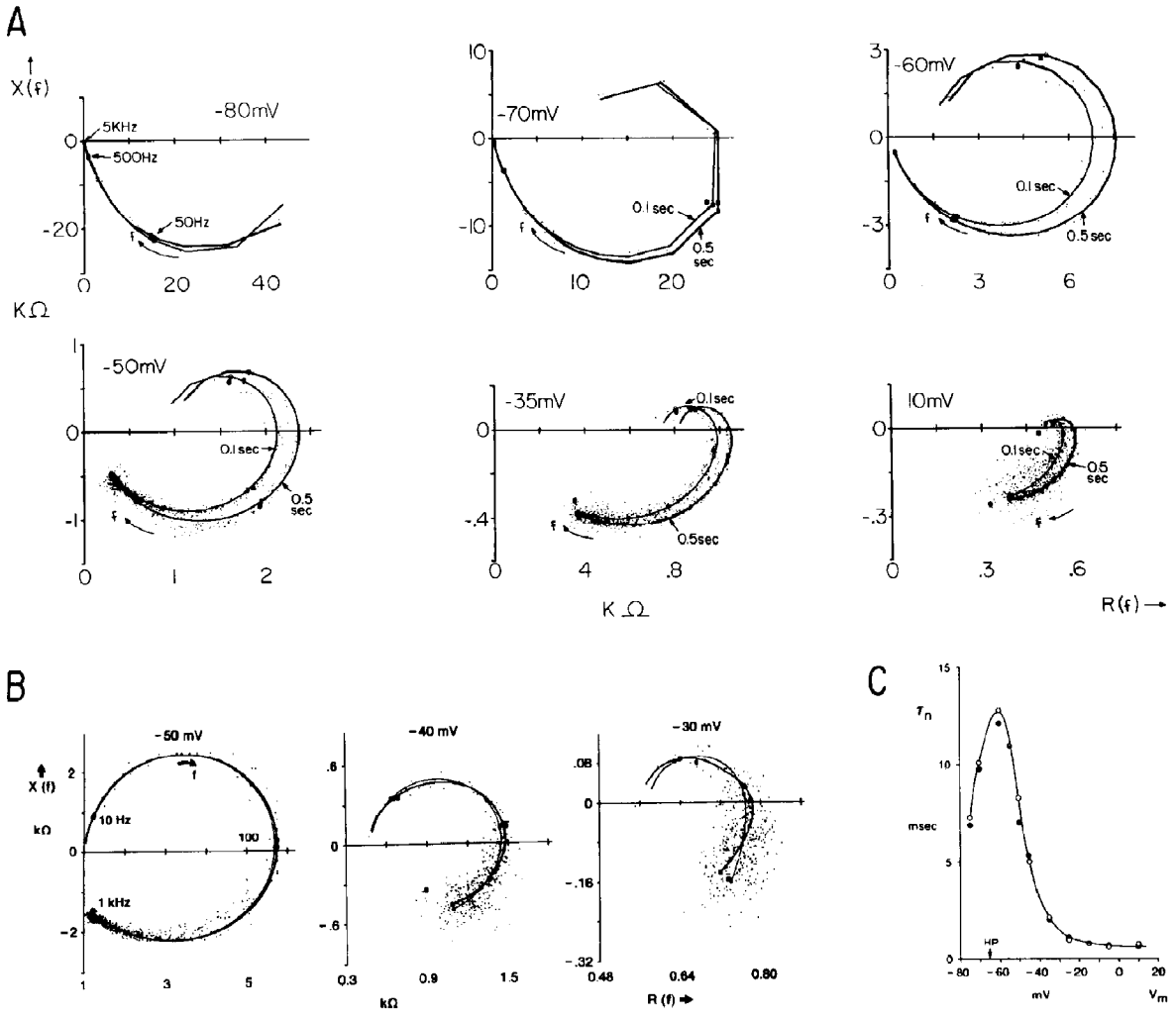

Fig. 4. (A) Pairs of impedance $[Z(jf) = R(f) + jX(f)]$ loci (400 frequency points) and curve fits (solid curves) of eq. 5 over the frequency range 12.5–5000 Hz plotted in the complex plane $[X(f)$ vs $R(f)]$. These data were acquired as rapid, complex admittance $[Y(jf)]$ data, as illustrated in fig. 3A, at premeasurement intervals of 0.1 and 0.5 s after step voltage clamps to each of the indicated membrane potentials from a holding of −65 mV. The impedance functions were formed from the reciprocal of the $Y(jf)$ determinations. Each curve fit is a best fit with all variables in eq. 5 freely determined. The near superposition and similarity in shape of the two loci at 0.1 and 0.5 s, at each potential, indicate that the admittance data reflect a steady state in this interval after step clamps. Axon 86–41 internally perfused with buffered KF and in ASW + TTX externally; 12°C; membrane area = 0.045 cm^2. (B) Admittance determinations in the frequency range 2.5–1000 Hz at three membrane potentials plotted in the complex impedance plane (points) and the best curve fits of a single relaxation-time model for $Y_K(jf)$ (eq. 7) (thin curves) and a two relaxation-time model (eq. 8) (thick curves) to the data. As shown in table 3 the χ^2 value for fits of the two-tau vs the one-tau model to these admittances and to those at other potentials in this axon were not generally better. Intact axon 86–61 in ASW + TTX (1 μM); 11.7° C. (C) K^+-conductance relaxation time as a function of voltage, $\tau_n(V)$, determined from the fits of the impedance data in panel A at two premeasurement intervals (fig. 3A) of 0.1 s (open circles) and 0.5 s (filled circles). The solid curve was drawn by eye. The closeness of the estimates of τ_n at each voltage indicates that the estimates from curve fits of the admittance determinations in panel A are time invariant. Thus, admittance determinations are in steady state in the interval 0.1–0.5 s after step clamps.

harmonic analysis to yield essentially a linear response in the squid axon. To satisfy criterion (ii), admittance data were acquired at 0.1 and 0.5 s after step voltage clamps to membrane potentials ranging from −80 to 10 mV. A representative set of these data is shown in fig. 4A in which the reciprocal of the admittance is plotted as 400-point impedance loci in the complex plane evaluated at the two times after steps to the indicated membrane voltages. The impedance loci at the two times show some differences at membrane voltages greater than −60 mV. However, best fits of eq. 5 (the solid curves) to these data yielded estimates of τ_n that were quite similar. Fig. 4C shows estimates of $\tau_n(V)$ from admittance data obtained in the frequency band 12.5–5000 Hz at the two acquisition times after step clamps. The estimated values at the different times (open vs filled symbols) are reasonably close. Similar results were obtained in eight other axons. Thus, the admittance appears to be sufficiently time invariant in the interval between 0.1 and 0.5 s after a step to consider the measurement to reflect a steady-state condition in this interval.

3.5. Comparison of τ_n estimates from small step vs admittance determinations

To ensure that admittance analysis yielded values of τ_n that were equivalent to the ones obtained in a small-step analysis, both types of measurements were made on the same axon over a 10 mV range from holding (−65 mV) and with the same premeasurement interval (0.2 s). A small step (1 mV) was superposed onto larger steps and applied 0.2 s after the onset of the large steps so that the response to the small step occurred in the same 'data acquired' interval as that of the admittance determination shown in fig. 3A. Small-step measurements at membrane potentials more positive than −50 mV were not useful due to the decay in the mean current response during the acquisition interval (see fig. 3A) which distorted the time course of the small step response. Table 1 contains the values obtained for τ_n from curve fits of the two types of data. Similar results were obtained in seven other axons. Except for the values at −55 mV, there is agreement within 2% at the other potentials, demonstrating the equivalence of the two determinations of τ_n over the limited potential range.

Table 1

Comparison of τ_n estimates from best fits of small step (1 mV) responses and complex admittances measured in the same time interval after clamp steps to the membrane voltage, V, in intact (not internally perfused) axon 86–52 in ASW + TTX (1 μM) at 13° C

V (mV)	τ_n		
	Small step (ms)	Admittance (ms)	Difference (%)
−65	8.7	8.8	1.1
−60	9.8	9.7	1.0
−55	11.3	11.7	3.5
−50	12.4	12.6	1.6

3.6. Bounds on the estimated values of τ_n from admittance analysis

Use of admittance analysis as a basis for judging whether an HH analysis is equivalent to a linear analysis assumes that the variation in admittance estimates of τ_n is less than the difference between the value of τ_n obtained from admittance vs HH analyses. To validate this assumption admittance measurements were made with the following protocol. At each membrane potential, eight separate admittance determinations were made. An average admittance was calculated by averaging the real and imaginary parts from the eight single determinations. At each frequency the real and imaginary parts (from each of the single admittance determinations that went into the average calculation) were used to calculate the standard deviation from the real and imaginary parts of the average admittance. Two new admittance functions were then generated by changing the real and imaginary parts of the average admittance at each frequency by plus or minus one standard deviation. By curve fits of eq. 5 to these three admittance functions at different voltages, three estimates of τ_n were obtained at each voltage. These results are provided in table 2. The differences in the values of τ_n listed in table 2 provide a measure of error (that includes the curve

Table 2

Variation in the estimates of τ_n from admittance determinations at membrane potential, V

Eq. 5 was fitted to the average of the real and imaginary parts of 8 single, admittance determinations at each voltage. The standard deviation of the real and imaginary parts of the single determinations from those of the average was calculated at each frequency of the average admittance. Two new admittance functions were generated and fitted by incrementing (+S.D.) or decrementing (−S.D.) the value of the real and imaginary parts of the average admittance at each frequency by one standard deviation. Intact axon 87–39 in ASW+TTX (1 μM) at 12.5°C.

V (mV)	τ_n (ms)		
	+S.D.	Average	−S.D.
−65	8.0	8.4	8.5
−60	8.8	8.9	8.9
−55	9.4	9.5	9.7
−50	9.3	9.4	9.4
−45	7.3	7.4	7.5
−40	6.2	6.4	6.5
−35	5.0	4.9	4.9
−30	3.4	3.4	3.5
−25	2.3	2.2	2.3

fitting process) associated with estimation of τ_n from the fitting of averaged admittance data. The variation in the estimate of τ_n from average admittances over the entire voltage range is less than 5% and thus, does not account for the difference in the admittance- and HH-derived curves in fig. 1. Consequently, the result that an HH analysis does not yield the same quantitative information as a linear analysis is unaffected by variations in the estimates of τ_n from admittance determinations.

3.7. Complications in interpreting HH- and admittance-derived kinetics due to K^+ accumulation and inactivation

Other possibilities that could lead to disagreement between HH- and admittance-analysis estimates of relaxation times are the additional complexity added to a description of K^+ conduction by K^+ accumulation in the periaxonal space between glia and axolemma [21,22] and the existence of K^+-conductance inactivation processes [23–25]. During a long duration step clamp to a membrane potential of 0 mV, the efflux of K^+ builds up to a steady value with a time constant of about 30 ms resulting in a periaxonal K^+ concentration change of about 80 mM [22]. The mean effect of K^+ accumulation appears to be distortion of the rising phase of outward i_K. This distortion produces an underestimate of τ_n by HH analysis at all voltages [22], which is not the case with respect to admittance estimates of τ_n with voltage (admittance-derived curves cross HH-derived curves in fig. 1). This result strongly suggests that the disagreement between HH and admittance estimates of τ_n is not due to K^+ accumulation effects. Most of the decaying phase of i_K during long-duration step clamps (fig. 3A) has been shown [23,24,26] to be a manifestation of a fast inactivation (relaxation time $\tau_i = 20$–30 ms) of K^+ conductance not accounted for in the HH formulation. Furthermore, the kinetics of K^+ conduction in the squid axon has been shown to be dependent on the external K^+ concentration [27,28]. These observations suggest that a comparison between early transient step responses and later steady-state admittances may yield different values for K^+-conductance kinetic parameters if these phenomena are discernible in admittance measurements. With respect to the present experiments, as already indicated, fits of the single relaxation-time model expressed in eqs 5–7 appeared to be good enough not to require an additional relaxing term.

To determine whether higher order kinetics of K^+ conduction are evident in steady-state admittances, a single-relaxation-time model expressed in eq. 7 and a two-relaxation-time model given by

$$Y_K(jf) = g_{K_\infty} + g_{K_1}(1 + j2\pi f\tau_n)^{-1} + g_{K_2}(1 + j2\pi f\tau_i)^{-1} \quad (8)$$

were used in conjunction with eqs 5 and 6 to fit the same set of admittance data. Fig. 4B shows curve fits (solid curves) of single (thin curves) and two (thick curves) relaxation time equations to representative admittance data (points) plotted in the complex impedance plane at three membrane potentials. Table 3 provides the results of the best fits of the data in fig. 4B and at other membrane potentials. The difference between the single- and two-tau fits (table 3) was not great but the χ^2 value obtained for two-tau fits was generally not

Table 3

Comparison of one- and two-relaxation-time model fits to the same set of complex admittance determinations

The χ^2 value was calculated on 48 points of data spanning the frequency range from 2.5 to 1000 Hz (86–61, 11.7 °C).

V (mV)	τ_n (ms)	χ^2 ($\times 10^{-7}$)	τ_n (ms)	τ_i (ms)	χ^2 ($\times 10^{-7}$)
−65	11.2	0.95	8.8	71.1	0.73
−55	15.0	2.91	10.1	18.1	2.37
−50	16.8	8.67	11.8	21.3	9.34
−45	17.9	32.3	10.5	23.2	31.1
−40	19.6	57.4	6.8	25.5	59.1
−35	17.6	47.6	5.8	25.0	48.1
−30	12.4	40.1	2.0	18.8	40.7
−25	5.2	41.0	1.2	28.7	40.0

better than for single-tau fits. As can be seen in fig. 4B, the fits of average admittance data with a single tau were reasonable with respect to the scatter, especially for large depolarizations (−30 mV, fig. 4B). Nevertheless, the two-tau estimates did give a second voltage-sensitive relaxation time, τ_i, that was in the 20–30 ms range reported by Inoue [23].

4. Discussion

4.1. HH analysis does not yield linear kinetic parameters

The original intent of Hodgkin and Huxley was to describe the individual ionic current flows that reflect the ion permeability changes underlying excitation (action potential generation) in a squid axon membrane. In successfully accomplishing this objective, they chose linear kinetics to describe the ion conductance rate processes. However, fits of nonlinear step-clamp responses were made by empirical determination of power-law relationships (e.g., eq. 1) between the conductances and parameters (e.g., eq. 4) associated with the assumed relaxation processes. Because the relaxation times and rate constants were defined at constant voltage in linear rate equations (e.g., eq. 2), in a vast, subsequent literature (see refs. 19 and 33) the presumption has been that application of the HH formulation to step-clamp data is analogous to a linear analysis of ion conduction. The comparison presented here between the relaxation times determined over a 60 mV range by admittance and HH analysis in the same axon do not support this premise.

In section 3, τ_n determinations from admittance analysis were shown to be equivalent to a small-step analysis and they were time invariant. Other explanations for the discrepancy between admittance and HH determinations of τ_n are possible. The HH analysis was performed on data acquired as transient responses immediately following a step change in membrane voltage whereas the admittance data were acquired in a steady state (0.2 s) after a step change. If K^+-conductance kinetics were time varying, the two sets of τ_n determinations would not necessarily agree.

As mentioned earlier (section 3), the effect of K^+ accumulation in the periaxonal space between Schwann cells and axolemma membranes [21] alters step-clamp responses [22]. Secondly, K^+ conductance inactivates with time following a step clamp. The inactivation occurs in two different time frames. A fast inactivation occurs with a relaxation time of 20–30 ms [23,24,26] and a slow inactivation develops with a relaxation time of tens of seconds [25]. These effects could account for the differences in the results of these experiments. However, in the potential range of small steps (< 10 mV), which elicit small currents and thus smaller ion accumulation effects and no apparent decaying phase in i_K due to inactivation, the discrepancy between the admittance- and HH-derived curves of fig. 1 is greatest. This suggests that an HH analysis does not yield the same values as an admittance analysis regardless of effects produced by K^+ accumulation or conductance inactivation. Furthermore, the differences between the values of τ_n from HH and admittance analysis over the voltage range examined were not consistent with underestimates at all voltages due solely to K^+ accumulation described by Adelman et al. [22]. The subsequent discussion focuses on aspects of an HH analysis that could account for the discrepancies in estimates of ion-conductance kinetic parameters from those obtained by direct linear analysis.

4.2. Sources of error in extracting linear kinetic parameters from an HH analysis

There are two types of problems in implementation of the HH methodology. The first involves data processing and the second is in the empirical selection of exponents for fits of the power-law relations to data. For step responses, the capacitive transient and leakage currents must be removed from the total current in order to begin curve fitting at the actual onset of the response, otherwise estimation of the best value for x cannot be made with sufficient accuracy. Errors in the temporal form of ionic current responses can arise from improper subtractions of leakage or capacitive transients from 'activating' responses.

In applying the power-law formulation previously, the selection of the best exponent, x, in eq. 4 to fit step-clamp responses has been an issue in the squid axon [29–31]. In more recent work, Gilly and Armstrong [32] found that an exponent of 6 gave a better fit than 4 for i_K responses (their fig. 11) for very large steps (110 mV — twice as large as the largest steps in this study) and with axons in high K^+ concentration ASW. Gilly and Armstrong also noted that the HH fits with $x = 4$ of large-step responses rose initially too slowly and subsequently too rapidly, as was our experience in fitting responses to smaller steps (fig. 2B). Moreover, their best fit was obtained when the rate constants for transitions between the first four steps of the K^+-channel kinetic scheme were equal and fast and the last step was slow (rate limiting). In effect, the exponent of 6 produced sufficient delay (time associated with transitions through the five nonconducting states prior to the transition to the conducting state) to allow fit of the rest of the response by a first-order response (the rate-limiting step). Nevertheless, the dependence of estimates of kinetic parameters on the selection of an appropriate exponent is a serious deficiency in the use of the HH empiricism and protocol as a way to obtain quantitative kinetic data.

Another possibility that might account for discrepancies in an HH analysis is associated with the use of large-step responses. Large steps excite nonlinear modes in the responses. Some of these modes may arise from nonlinear phenomena unrelated to the kinetics of ion channels. Consequently, fits of these nonlinear responses with the HH empirical formalism, within which are contained linear kinetic parameters, could result in estimates of linear kinetic parameters that are in error due to the distortion produced by fitting unrelated nonlinear modes.

4.3. Analysis of rapid admittance determinations — a way to assess the macrokinetics of membrane conduction

Finally, rapid admittance measurements merit usage as a means of characterizing the linear kinetics of ion conduction processes in membranes. Data manipulations (corrections for capacitance, leakage and series resistance) that are associated with analysis of step-clamp responses are not required, and membrane admittances are acquired almost as quickly. Furthermore, analysis of admittances provides estimates of linear kinetic parameters that do not depend on empiricism. The main disadvantage of the method is that more parameters (for capacitance, leakage and series resistance) are necessary in modeling and curve fitting admittance functions. Alternatively, the effect of capacitance, series resistance and leakage can be removed from the total membrane admittance by vector subtraction of admittance functions obtained during membrane conditions in which all other conduction is suppressed [7]. In such cases the resultant admittance becomes the complex conductance (see eq. 8) of the ion conduction process under study and, for a single-relaxation-time model, requires only three parameters for fitting. Rapid admittance determinations can even be made during current transients; however, interpretations of admittance data not obtained in a steady state are not straightforward. The main advantage of recent advances in the speed with which admittance determinations can be made is that analysis of admittance functions provides an alternative comprehensive way to characterize linear or linearizable conduction systems in membranes over a wide range of experimental conditions. These data are fundamental in

the sense that they can be used as a basis for comparison of all linear models.

Acknowledgements

We thank Dr K.P. Tewari for help with the data analysis. This work was supported in part by Office of Naval Research Grant N00014-90-J-1137. We thank the Marine Biological Laboratory, Woods Hole, MA, for use of facilities.

References

1 A.L. Hodgkin and A.F. Huxley, J. Physiol. 117 (1952) 500.
2 Y. Husimi and A. Wada, Rev. Sci. Instrum. 47 (1976) 213.
3 D. Poussart and U.S. Ganguly, Proc. IEEE 65 (1977) 741.
4 H.M. Fishman, L.E. Moore and D. Poussart, in: The biophysical approach to excitable systems, eds W.J. Adelman, Jr and D.E. Goldman (Plenum, New York, 1981) p. 65.
5 G. Kottra and E. Fromter, Pflügers Arch. 402 (1984) 409.
6 H.M. Fishman, H.R. Leuchtag and L.E. Moore, Biophys. J. 43 (1983) 293.
7 H. Hayashi and H.M. Fishman, Biophys. J. 53 (1988) 747.
8 B. Sakmann and E. Neher, Single-channel recording (Plenum, New York, 1983).
9 D. Colquhoun and A.G. Hawkes, in: Single-channel recording, eds B. Sakmann and E. Neher (Plenum, New York, 1983) p. 135.
10 F. Sachs and M. Sokabe, Biophys. J. 57 (1990) 265a.
11 H.M. Fishman, Prog. Biophys. Mol. Biol. 46 (1985) 127.
12 W.K. Chandler, R. FitzHugh and K.S. Cole, Biophys. J. 2 (1962) 105.
13 A. Mauro, F. Conti, F. Dodge and R. Schor, J. Gen. Physiol. 55 (1970) 496.
14 S. Miyamoto and H.M. Fishman, Ferroelectrics 86 (1989) 129.
15 H.M. Fishman and R.J. Lipicky, Biophys. J. 51 (1987) 51a.
16 H.M. Fishman and R.J. Lipicky, Proc. 9th Ann. Conf. IEEE-EMBS 1 (1987) 57.
17 H. Nakamura, Y. Husimi, G.P. Jones and A. Wada, J. Chem. Soc. Faraday Trans. II 73 (1977) 1178.
18 L.E. Moore, H.M. Fishman and D. Poussart, J. Membrane Biol. 54 (1980) 157.
19 K.S. Cole, Membranes, ions and impulses (University of California Press, Los Angeles, 1972).
20 P.R. Bevington, Data reduction and error analysis of the physical sciences (McGraw Hill, New York, 1969).
21 B. Frankenhaeuser and A.L. Hodgkin, J. Physiol. 131 (1956) 341.
22 W.J. Adelman, Jr, Y. Palti and J.P. Senft, J. Membrane Biol. 13 (1973) 387.
23 I. Inoue, J. Gen. Physiol. 78 (1981) 43.
24 L.D. Chabala, J. Physiol. 356 (1984) 193.
25 G. Ehrenstein and D.L. Gilbert, Biophys. J. 6 (1966) 553.
26 I. Inoue, J. Gen. Physiol. 88 (1986) 507.
27 R.P. Swenson and C.M. Armstrong, Nature 291 (1981) 427.
28 J.R. Clay, Biophys. J. 50 (1986) 197.
29 K.S. Cole and J.W. Moore, Biophys. J. 1 (1960) 161.
30 R. FitzHugh, J. Cell. Comp. Physiol. 66 (1965) 111.
31 C.M. Armstrong, J. Gen. Physiol. 54 (1969) 553.
32 W.F. Gilly and C.M. Armstrong, J. Gen. Physiol. 79 (1982) 965.
33 H. Meves, in: The squid axon, ed. P.F. Baker, in: Current topics in membrane transport (Academic Press, New York, 1984) p. 279.